The ClC-3 chloride channel promotes acidification of lysosomes in CHO-K1 and Huh-7 cells

XINHUA LI,[1] TING WANG,[1] ZHIFANG ZHAO,[1] AND STEVEN A. WEINMAN[1,2]
[1]*Department of Physiology and Biophysics and* [2]*Department of Internal Medicine,*
University of Texas Medical Branch, Galveston, Texas 77555

Li, Xinhua, Ting Wang, Zhifang Zhao, and Steven A. Weinman. The ClC-3 chloride channel promotes acidification of lysosomes in CHO-K1 and Huh-7 cells. *Am J Physiol Cell Physiol* 282: C1483–C1491, 2002. First published February 13, 2002; 10.1152/ajpcell.00504.2001.—ClC-3 is a voltage-gated Cl^- channel that is highly conserved and widely expressed, although its function, localization, and properties remain a matter of considerable debate. In this study, we have shown that heterologous expression of ClC-3 in either Chinese hamster ovary (CHO-K1) or human hepatoma (Huh-7) cells results in the formation of large, acidic vesicular structures within cells. Vesicle formation is prevented by bafilomycin, an inhibitor of the vacuolar ATPase, and is not induced by an E224A mutant of ClC-3 with altered channel activity. This demonstrates that vesicle formation requires both proton pumping and Cl^- channel activity. Manipulation of the intracellular Cl^- concentration demonstrated that the ClC-3-associated vesicles shrink and swell consistent with a highly Cl^--permeable membrane. The ClC-3 vesicles were identified as lysosomes based on their colocalization with the lysosome-associated proteins lamp-1, lamp-2, and cathepsin D and on their failure to colocalize with fluorescently labeled endosomes. We conclude that ClC-3 is an intracellular channel that conducts Cl^- when it is present in intracellular vesicles. Its overexpression results in its appearance in enlarged lysosome-like structures where it contributes to acidification by charge neutralization.

endosomes; bafilomycin; ClC channels

CL^- CHANNELS are present in all cells both at the plasma membrane and in intracellular sites. They are involved in diverse cell functions including stabilization of membrane potential, transepithelial transport, maintenance of intracellular pH, and cell volume regulation (14, 15). Some Cl^- channel functions have been associated with specific channel molecules. For example, ClC-1 is a myocyte plasma membrane channel that regulates membrane potential (33, 38), and ClC-5 is an endosomal Cl^- channel that participates in acidification and endocytosis (29, 34). However, for many Cl^- channels, it has not been possible to associate molecular identity with function (19). In hepatocytes, as yet unidentified Cl^- channels participate in cell volume

regulation (1, 7, 22, 23) and acidification of intracellular organelles (5, 24, 28, 36).

The ClC Cl^- channel family has proven to be important in diverse cellular functions (10, 14, 40). In this family, ClC-3, along with the highly homologous ClC-4 and ClC-5, form one distinct branch. Each has been functionally expressed, and all possess similar channel properties (8, 20). ClC-5 localizes in endocytic vesicles in the kidney where it is necessary for acidification and endocytosis (12, 29). The precise function of ClC-3 is controversial. Although it was first proposed as a swelling-activated Cl^- channel in plasma membranes (3), recent studies support a predominantly intracellular localization (20, 39). In knockout mice, Stobrawa et al. (35) found that disruption of the ClC-3 gene impaired acidification of synaptic vesicles in hippocampal neurons. However, ClC-3 is highly conserved and broadly distributed, and its functions may not be limited to acidification of synaptic vesicles.

We have previously cloned ClC-3 from rat hepatocytes and have characterized its channel activity (20, 32). In the present study, we have expressed ClC-3 in human hepatoma (Huh-7) and Chinese hamster ovary (CHO-K1) cells and noted that ClC-3 expression induced formation of large intracellular vesicles. ClC-3 protein localized abundantly in the vesicular membranes. Further examination revealed that ClC-3 functions as an intracellular Cl^- channel in these vesicles, cooperating with vacuolar H^+-ATPase to achieve H^+ and Cl^- flux. Our results provide direct evidence that ClC-3 is a functional intracellular channel and demonstrate the importance of ClC-3 in organelle acidification.

METHODS

ClC-3 expression vectors. Four different ClC-3 constructs were used. pClC3sFlag (short form) and pClC3lFlag (long form) were constructed in pcDNA 3.1 as described previously (20, 32). pClC3sGFP was prepared by subcloning the ClC-3 short form open reading frame into pEGFP-N1 (Clontech) between the *Xho*I and *Bam*H1 sites. This construct produced a fusion protein with the enhanced green fluorescent protein (EGFP) moiety attached to the COOH terminus of ClC-3. A pClC3sFlag E224A mutation was produced by using the

QuikChange site-directed mutagenesis kit (Stratagene). All constructs were confirmed by sequencing in the Protein Chemistry Laboratory of the University of Texas Medical Branch.

Cell culture and transfection. CHO-K1 or Huh-7 cells were cultured in DMEM/F-12 medium (Mediatech) and grown on glass coverslips in six-well plates. Cells were transiently transfected at 50–70% confluence with pClC3sFlag, pClC3lFlag, pClC3sGFP, or pClC3sFlag E224A by using Fu-GENE6 (Boehringer Mannheim) or Lipofectamine Plus (Life Technologies) following the manufacturer's protocol. Cells were used for experiments 48–72 h after transfection.

For patch-clamp experiments, cells were transfected with a mixture of either pClC3sFlag or its E224A mutant plus a GFP plasmid (pEGFP; Clontech) at a 30:1 ratio and observed under epifluorescence microscopy 48–72 h after transfection. Fluorescent cells were chosen for patch-clamp analysis.

Electrophysiology. Whole cell current recordings of ClC-3-expressing cells were performed by using a patch-clamp system (Axopatch-200 and pCLAMP v6.03, Axon Instruments) at room temperature (23°C) as described previously (20). The bath solution consisted of (in mM): 114 NaCl, 5.4 CsCl, 1 $MgSO_4$, 1.5 $CaCl_2$, 10 HEPES, and 10 glucose. Osmolality (measured with a vapor pressure osmometer, model 5500, Wescor, Logan, UT) was adjusted to 300 mosmol/kg H_2O by adding sucrose, and pH was adjusted to 7.4 with NaOH. Pipette solution contained (in mM) 120 CsCl, 3 $MgSO_4$, 1 $CaCl_2$, 11 EGTA, 3 Na_2ATP, 10 HEPES, and 10 glucose and was adjusted to pH 7.2 with CsOH. Osmolality was 290 mosmol/kg H_2O.

Immunofluorescence. Immunofluorescence was performed as described previously (32). Transfected cells were grown on glass coverslips. They were fixed with methanol at −20 °C for 10 min, washed in PBS, and incubated with the m2 anti-FLAG monoclonal antibody (1:500, Sigma) in 10% goat serum for 1.5 h. Coverslips were then washed for 2 h in PBS and incubated with Alexa Fluor 488-conjugated goat anti-mouse IgG (1:500, Molecular Probes) for 1 h followed by another hour of washing. Similar immunostaining was performed with primary antibodies against Golgi marker 58k protein (1:100, Abcam), human cathepsin D (1:100, Upstate Biotechnology), anti-lamp-1 monoclonal antibody H4A3, and anti-lamp-2 monoclonal antibody H4B4 (each at 1:200, Developmental Studies Hybridoma Bank, University of Iowa). Secondary antibodies were Alexa Fluor 594-conjugated goat anti-mouse IgG or Alexa Fluor 594 goat anti-rabbit IgG (1:500, Molecular Probes). Nuclear staining was performed with 4,6-diamidino-2-phenylindole (DAPI) dye as described previously (18). Cells were observed in a Nikon Eclipse 800 (Melville, NY) epifluorescence microscope with the FITC-filter set (excitation 465–495 nm, dichroic mirror 505 nm, emission 515–555 nm) for Alexa Fluor 488 conjugates, Texas red filter set (excitation 540–580 nm, dichroic mirror 595 nm, emission 600–660 nm) for Alexa Fluor 594 conjugates, and the DAPI filter set (excitation 340–380 nm, dichroic mirror 400 nm, emission 435–485 nm) for the nuclear DAPI dye. Images were acquired by using a Dage-MTI (Michigan City, IN) camera for later processing by Adobe Photoshop software.

Identification of acidic intracellular compartments. After transfection of pClC3sGFP for 48 h, LysoSensor blue DND-167 (Molecular Probes) was added to the medium to a final concentration of 1 μM and incubated for 30 min. Cells on coverslips were directly observed under the microscope with the FITC filter set for ClC-3 protein or DAPI filter set for LysoSensor. Images were recorded immediately to avoid photobleaching.

Examination of fluid-phase endocytosis. Cells grown on small coverslips were washed with HEPES-buffered saline solution (HBSS, in mM: 150 NaCl, 0.8 $MgSO_4$, 2.2 D-gluconic acid, hemicalcium salt, 4.2 K-gluconic acid, 10 HEPES, and 18 glucose, adjusted to pH 7.4 with NaOH) and incubated with Alexa Fluor 594-conjugated dextran (MW 10,000, Molecular Probe) at 5 mg/ml for 10 min. Dextran was removed by washing three times with HBSS, and the cells were subsequently incubated for variable times in the same solution before fixation with 3% paraformaldehyde. They were then washed in PBS and observed by epifluorescence microscopy.

Live-cell fluorescence microscopy. Cells transfected with pClC3sGFP were placed in a 0.5-ml thermostatic chamber (36°C) and perfused continuously at 2 ml/min with Cl^--free or Cl^--containing solutions. Epifluorescence images were acquired with a Nikon Eclipse TE200 inverted microscope using a ×60, 1.40 N.A. objective and Metamorph software. Cl^--containing isotonic solution was HBSS. Cl^--free solution used Na-gluconate to substitute the NaCl. Hypotonic solutions were prepared by reducing NaCl or Na-gluconate to 100 mM.

Materials. Bafilomycin A1 and DAPI were purchased from Sigma. Other chemicals were from Sigma or Fisher Scientific unless noted otherwise.

Data analysis. Assessment of the presence of vesicular structures in cells was performed by selecting four corner fields and a central field on each coverslip and scoring each fluorescent cell for the presence or absence of vesicles as assessed visually by a blinded observer. Transfection efficiency was also estimated each time. Statistical significance was tested using the χ^2 method.

RESULTS

ClC-3 expression induces the formation of intracellular vesicles. Huh-7 hepatoma cells and CHO-K1 cells were transiently transfected with pClC3sFlag or pClC3sGFP as described in METHODS. Neither of these tags at the COOH terminus affected channel properties (20). A consistent observation was that ClC-3 expression resulted in the formation of large intracellular vesicles, as shown in Fig. 1A. The vesicles themselves appeared to contain ClC-3 in their membranes. This phenomenon was observed in both CHO-K1 and Huh-7 cells. Similar vesicles could be observed with difference-interference contrast optics after transfection of untagged ClC-3 as well. In nontransfected or GFP only-transfected cells, the distinctive vesicles were never seen. This pattern of vesicle formation was specific to the short form of ClC-3 and was not seen with ClC-3 long form (Fig. 1B).

To determine the characteristics of these vesicles, we examined their internal pH in living cells. This was accomplished by exposing transfected cells to LysoSensor blue, a membrane-permeable weak base with an acid-dependent fluorescence (pKa 5.1). This molecule is useful for identification of acidic compartments because it is selectively concentrated in acidic spaces where its fluorescence quantum yield is dramatically increased. In practice, its blue fluorescence can only be observed in highly acidic spaces (21). After LysoSensor was incubated with pClC3sGFP-transfected cells for 30 min, the lumen of the vesicles exhibited very strong blue fluorescence (Fig. 2). Nontransfected cells gener-
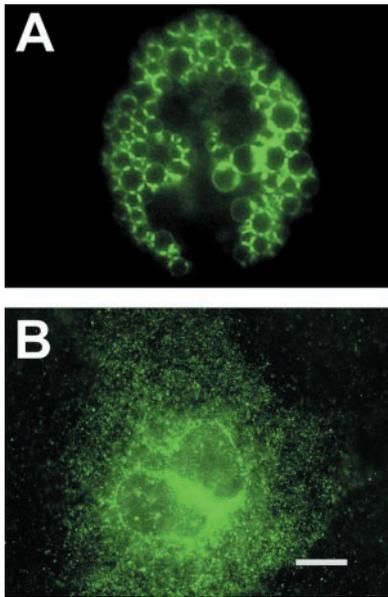
Fig. 1. Pattern of ClC-3 localization in human hepatoma (Huh-7) cells. *A*: cells were transfected with pClC3sGFP, fixed, and observed by epifluorescence microscopy as described in METHODS. ClC-3-GFP fluorescence is represented in green. Note the appearance of large vesicular structures. *B*: cells were transfected with pClC3lGFP (long form). Note the absence of large vesicles. Bar, 10 μm.

ally demonstrated small blue fluorescent spots, but these were dramatically smaller and less intense than in the transfected cells and were not visible under the imaging conditions used in Fig. 2. This demonstrates that the ClC-3-associated vesicles have a strongly acidic interior, whereas untransfected cells lack such large acidic compartments.

Vacuolar proton-ATPase is essential for the formation of ClC-3-associated vesicles. We hypothesized that abnormally large Cl⁻ conductance in association with

proton pumping from the vacuolar proton-ATPase might lead to vesicle enlargement by the accumulation of osmotically active Cl⁻ ions in the vesicle lumen. We then determined whether proton pumping was necessary for the formation of the enlarged structures. Figure 3 demonstrates that inhibition of the V-type ATPase (V-ATPase) with bafilomycin A1, a highly specific inhibitor of vacuolar proton-ATPase, nearly abolished formation of enlarged vesicles. ClC-3 was still abundantly expressed, but it was now located primarily in punctate spots without a discernable lumen. This indicates that vesicle enlargement requires proton pumping.

A ClC-3-channel mutation disables vesicle formation. As previously reported (20), expression of ClC-3 in CHO-K1 cells results in a strongly outward-rectifying Cl⁻ current, presumably because a fraction of the expressed ClC-3 also appears on the plasma membrane. To determine whether vesicle formation requires the channel activity of ClC-3, we introduced an E224A mutation in pClC3sFlag. This mutation corresponds to a highly conserved segment that lines the permeation pore of ClC channels (6) and forms part of the selectivity filter (4). The identical mutation in ClC-4 and ClC-5 dramatically changed channel conductance and rectification (8). Figure 4 demonstrates that the E224A mutation in ClC-3 produced the identical effect on ClC-3 voltage dependence as it did for ClC-4 and ClC-5. The mutant whole cell currents are largely inward rectifying and have reduced maximal conductance.

Transfection of CHO-K1 cells with wild-type or E224A constructs resulted in nearly identical transfection efficiency (24.0 vs. 22.3%), and comparable amounts of protein appeared to be present on immu-
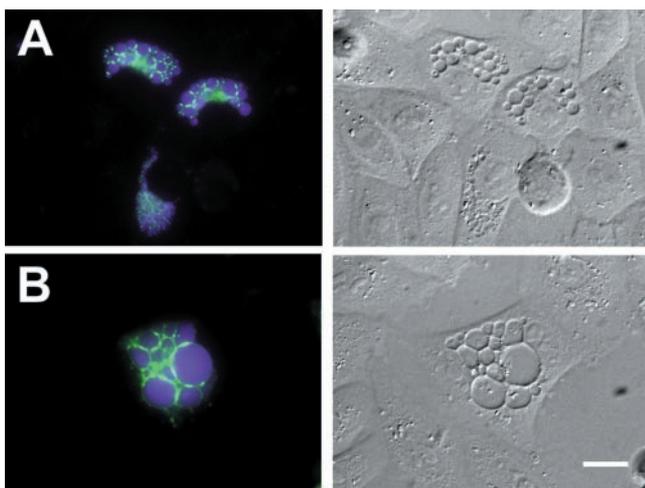

Fig. 2. Acidic lumen in ClC-3-associated vesicles. Chinese hamster ovary (CHO-K1) (*A*) or Huh-7 (*B*) cells were transfected with pClC3sGFP. Transfected cells were incubated with LysoSensor blue for 30 min and then observed without fixation. Images displayed (*left*) are composites of LysoSensor fluorescence and ClC-3-GFP fluorescence (green). A transmitted light image (*right*) using Nomarski optics is also shown for each image. Bar, 10 μm.
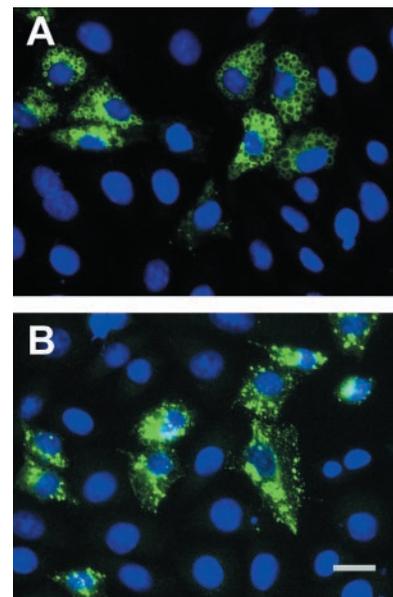

Fig. 3. Effect of bafilomycin on vesicle formation. CHO-K1 cells were transfected with pClC3sFlag and incubated with bafilomycin (10 nM) for 8 h. Cells were fixed and stained with anti-FLAG antibody, Alexa-488 goat anti-mouse secondary antibody, and DAPI stain to visualize the nuclei. *A*: control without bafilomycin. *B*: after bafilomycin incubation. Bar, 20 μm.
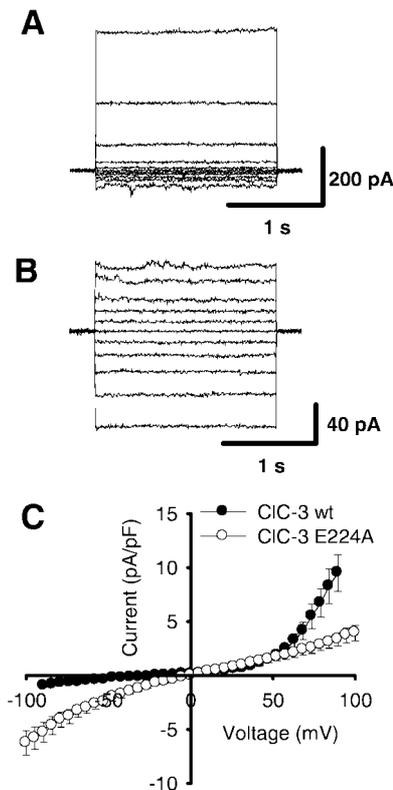
Fig. 4. Conductive properties of ClC-3 E224A channel mutant. CHO-K1 cells were transfected with either pClC3sFlag or pClC3sFlag-E224A. Currents were recorded after 48 h by whole cell patch clamp using 2-s voltage pulses and 20-mV increments from −100 to 100 mV for wild-type ClC-3 (*A*) or E224A mutant (*B*). Current-voltage relationships for a voltage ramp from −100 to 100 mV are displayed in *C*. Control, $n = 5$; E224A, $n = 8$.

(20, 23, 30) and allows exchange of intracellular and bath Cl^-. Figure 6, *A*–*C*, shows a representative series of images obtained with this protocol. Within 10 min of exposure to Cl^--free solution, vesicles were notably smaller (Fig. 6, *A* vs. *B*). By 20 min (Fig. 6*C*), the vesicles appeared as punctate spots and no open lumen could be observed. Conversely, when cells were preincubated for 2 h in Cl^--free solution, the ClC-3-containing structures appeared as punctate spots or small vesicles only. Upon reexposure to Cl^--containing solutions, the vesicles markedly expanded within 30 min (Fig. 6, *D*–*F*). In some cases, both shrinkage and expansion could be observed in the same cell, although this latter protocol required longer incubation times (>60 min), and repeated exposure to light during this period frequently resulted in cell death before the end of the protocol. In control experiments in which either Cl^--containing or Cl^--free solution was maintained for 30 min, there was no change in vesicle size. Cl^--dependent shrinkage and expansion of vesicles was observed in seven different cell preparations, and in
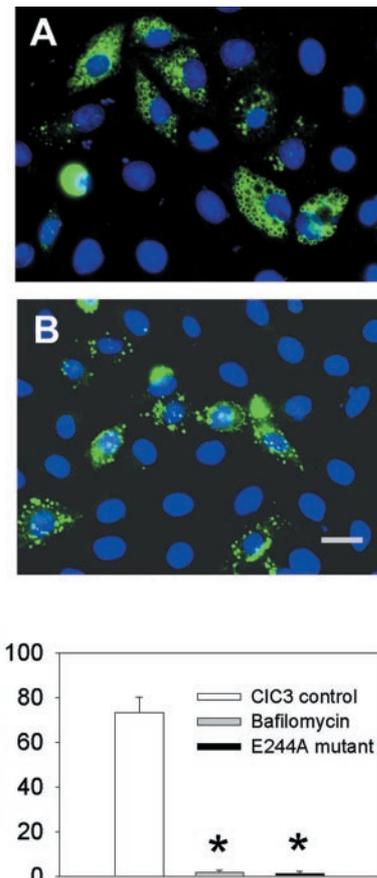
nofluorescent images (Fig. 5). Strikingly, the E224A mutant protein failed to expand intracellular vesicles, and its intracellular distribution in punctate spots without a discernable lumen was almost identical to that seen in the presence of bafilomycin. The effects of bafilomycin and the E224A mutant on vesicle formation are summarized in Fig. 5*C*.

ClC-3-mediated Cl− flux across the vesicle membrane. To determine whether the ClC-3-associated vesicles possess high Cl^- conductance, we manipulated Cl^- gradients across the vesicle membrane and recorded resulting changes in vesicle size. Live cells expressing the ClC-3-GFP-fusion protein were observed by epifluorescence microscopy, superfused with Cl^--free solution, and then returned to normal Cl^- bath solution. Preliminary studies, however, showed that the plasma membrane was relatively impermeable to Cl^-, and therefore changes in bath Cl^- concentration only slowly affected the gradients across the membrane of the intracellular vesicles.

To circumvent this problem, we superfused cells with Cl^--containing solutions and then abruptly changed to Cl^--free bathing solution. Shortly after the change to Cl^--free solution, cells were exposed to a hypotonic, Cl^--free bath for 3 min. This treatment transiently activates plasma membrane Cl^- channels

Fig. 5. Effect of E224A mutation on the ClC-3-associated vesicles in CHO-K1 cells. CHO-K1 cells were transfected with either pClC3sFlag (*A*) or pClC3sFlag-E224A (*B*) and subsequently fixed and stained as in Fig. 3. Bar, 20 μm. *C*: images obtained as displayed in *A* and *B* and in Fig. 3 were assessed for the number of ClC-3-expressing cells with visible vesicles. Control, $n = 202$ cells in 5 coverslips; bafilomycin, $n = 200$ cells in 6 coverslips; E224A mutant, $n = 221$ cells in 6 coverslips. *$P < 0.01$ by χ^2 analysis. Values are means ± SE derived from the percentage of vesicle-containing cells on each coverslip.
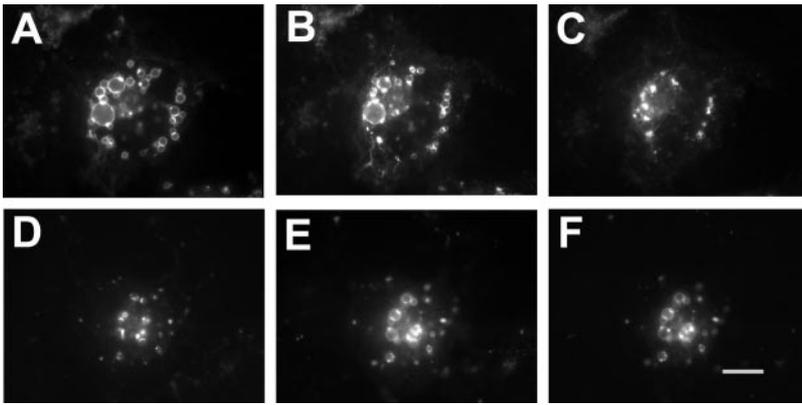
Fig. 6. Cl⁻-dependent volume changes of the ClC-3-associated vesicles. *A–C*: Huh-7 cells transfected with pClC3sGFP were equilibrated in Cl⁻-containing medium and exposed to Cl⁻-free solution at *time* 0 ($t = 0$). A 3-min exposure to hypotonic Cl⁻-free solution occurred at the beginning of this interval. *A*: $t = 0$ min; *B*: $t = 10$ min; *C*: $t = 20$ min. Note the progressive shrinkage of the ClC-3-containing vesicles. *D–F*: cells were incubated for 2 h in Cl⁻-free solution and returned to Cl⁻-containing medium at *time* 0. *D*: $t = 0$ min; *E*: $t = 30$ min; *F*: $t = 40$ min. Note the progressive swelling of the ClC-3-containing structures. Bar, 10 μm.

each case similar reversible Cl⁻-dependent changes in vesicle size were observed.

ClC-3 vesicles are lysosomes. ClC-3-expressing cells were fixed and immunostained with marker antibodies as described in METHODS. Figure 7, *A–C*, demonstrates that ClC-3 expressed in Huh-7 cells did not colocalize with a Golgi marker (Golgi 58K protein). However, the lumen of many of the vesicular structures demonstrated the presence of cathepsin D (Fig. 7, *D–F*), a lysosome-specific protease, suggesting that some of these enlarged ClC-3-containing structures may be lysosomes. This was further confirmed by the demonstration that both lysosome-associated membrane proteins lamp-1 and lamp-2 (9) strongly colocalize with ClC-3
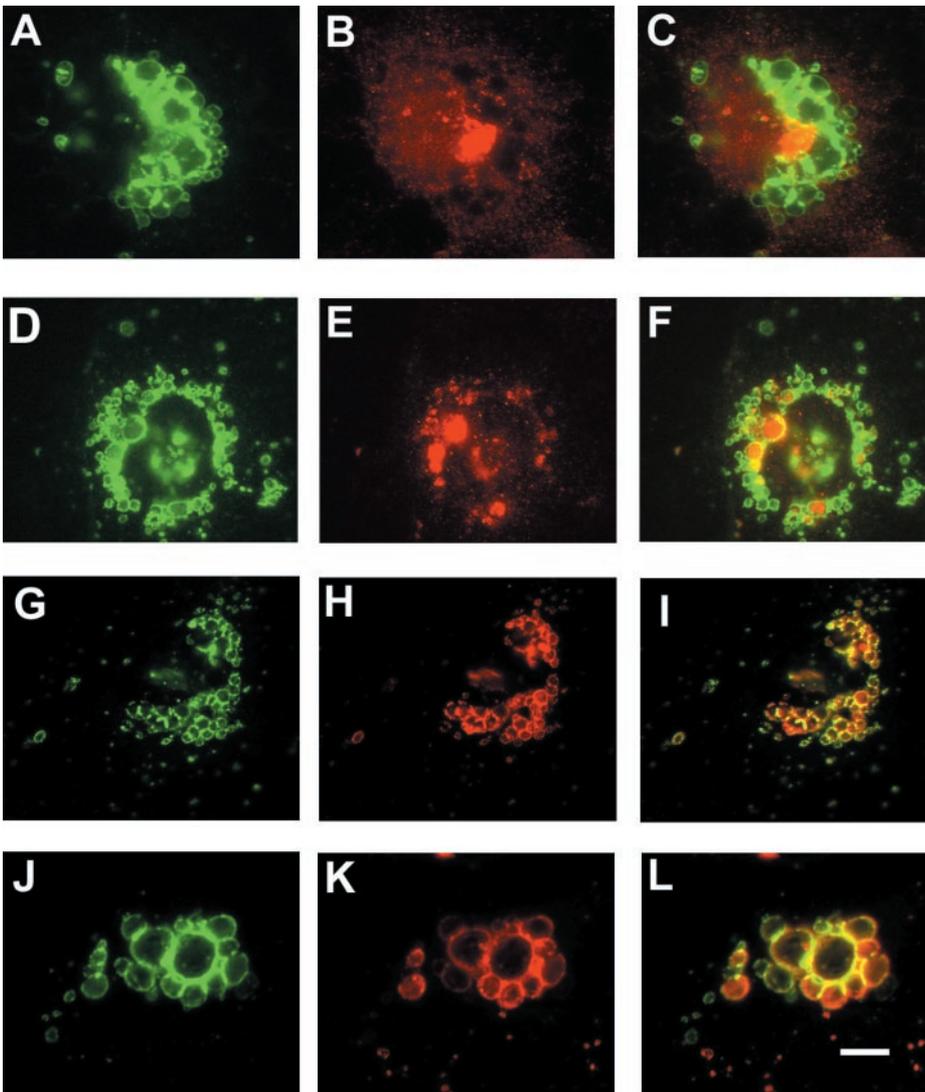

Fig. 7. Colocalization of ClC-3 with marker proteins. Huh-7 cells were transfected with pClC3sGFP, fixed, and immunolabelled with anti-Golgi 58K (*A–C*), anticathepsin D (*D–F*), anti-lamp-1 (*G–I*), or anti-lamp-2 (*J–L*) primary antibodies. Alexa-594 goat anti-mouse IgG was the secondary antibody. The fluorescent images of ClC-3-GFP (green, *A*, *D*, *G*, and *J*) or marker protein (red; *B*, *E*, *H*, and *K*) are displayed along with the respective composite images (*C*, *F*, *I*, and *L*). Areas of colocalization appear yellow in the composite images. Bar, 10 μm.

(Fig. 7, *G–L*). Similar results were obtained in CHO-K1 cells (data not shown).

Lamp-1 and lamp-2 can be present in late endosomes in addition to lysosomes. To determine whether these vesicles represent lysosomes as opposed to endosomes, we examined the time course of appearance of a fluid-phase marker into the vesicles. The results (Fig. 8) demonstrate that fluorescent dextran is taken up into small endocytic vesicles that distribute throughout the cell. After a chase period of 10–15 min (Fig. 8, *A* and *D*) or 35 min (Fig. 8, *B* and *E*), dextran did not appear within the ClC-3 vesicles. However, after a chase period of 1.5 h, the fluorescent dextran was found completely within the ClC-3-containing structures. This delayed appearance of endocytosed dextran into the ClC-3 vesicles suggests that they are lysosomes and not early or late endosomes.

DISCUSSION

The functions and properties of ClC-3 have been difficult to determine. ClC-3 has variously been proposed to be a swelling-activated plasma membrane Cl^- channel, a Ca^{2+}-activated channel, and an intracellular channel necessary for acidification of synaptic vesicles (3, 13, 35). We have previously determined that

Fig. 8. Colocalization of ClC-3 with endocytosed fluorescent dextran. CHO-K1 (*A*–*C*) or Huh-7 cells (*D*–*F*) were transfected with pClC-3sGFP and subsequently exposed to fluorescent dextran for 10 min. They were subsequently washed and incubated at 36°C in dextran-free solution for 10–15 min (*A*, *D*), 35 min (*B*, *E*), or 1.5 h (*C*, *F*). The relationship of ClC-3 fluorescence (green) and dextran fluorescence (red) is shown in each image. Areas of colocalization appear yellow. Bar, 10 μm.

ClC-3 Cl^- currents are different from swelling-activated Cl^- currents and have nearly identical biophysical properties as ClC-5 (20).

In the present study, we have shown that a single amino acid substitution at position 224 of ClC-3 produced the same effect on channel properties as does the corresponding mutation in ClC-4 and ClC-5 (8). This definitively confirms that the ClC-3 molecule itself mediates the channel activity that we have observed here and in our previous study (20). Furthermore, expression of ClC-3 in CHO-K1 or Huh-7 cells results in the development of large intracellular vesicular structures with the ClC-3 molecules localized in the vesicular membrane. The vesicles possess high Cl^- permeability, and the interior pH of these vesicles was <5.1 as assessed by Lysosensor blue. Expansion of these ClC-3-associated vesicles was dependent on both proton pumping and normal ClC-3 channel activity. These findings strongly support the conclusion that ClC-3 is an intracellular Cl^- channel that participates in vesicular acidification.

Our data demonstrate that the large ClC-3 vesicular structures have the properties of lysosomes. Although they are larger than normal lysosomes, they contain the lysosomal membrane proteins lamp-1 and lamp-2, as well as the lysosomal protease cathepsin D. In addition, endocytosed dextran colocalizes with them only at times >1 h postinternalization, a time at which endosomal contents have been delivered to lysosomes (31). This pattern shows that the ClC-3 vesicles are not endosomes but rather lysosomes. It is important to note, however, that the distinction between late endosomes and lysosomes may be difficult to establish, and hybrid organelles may also exist (25). In addition, not all expressed ClC-3 is present in these enlarged lysosomal structures, and other sites of localization may occur as well.

Multiple organelles require an acidic environment for proper functioning. This is achieved by an electrogenic vacuolar H^+-ATPase that actively transports protons from the cytosol into the vesicle lumen (11, 27, 37). Efficient pumping requires charge neutralization by Cl^- flux into the lumen where the steady-state pH depends on the balance of proton pumping, Cl^- permeability, and proton leakage. This acidification process may promote enlargement of the luminal size by translocation of Cl^- ions and also by the trapping of basic osmolytes (37). Overexpression of ClC-3 in lysosomes may thus be responsible for both abnormal enlargement and hyperacidification.

The precise properties of ClC-3 are the subject of dispute, and different laboratories appear to have obtained conflicting results with this channel. We believe that our present results may shed some insight on the reasons for these differences. Our laboratory has previously reported whole cell currents associated with expression of both the short and long form of ClC-3 (32). The mutation results presented in Fig. 4 clearly show that these short form-associated currents are mediated by ClC-3. The current has extreme outward rectification, is insensitive to NPPB [5-nitro-2-(3-phe-
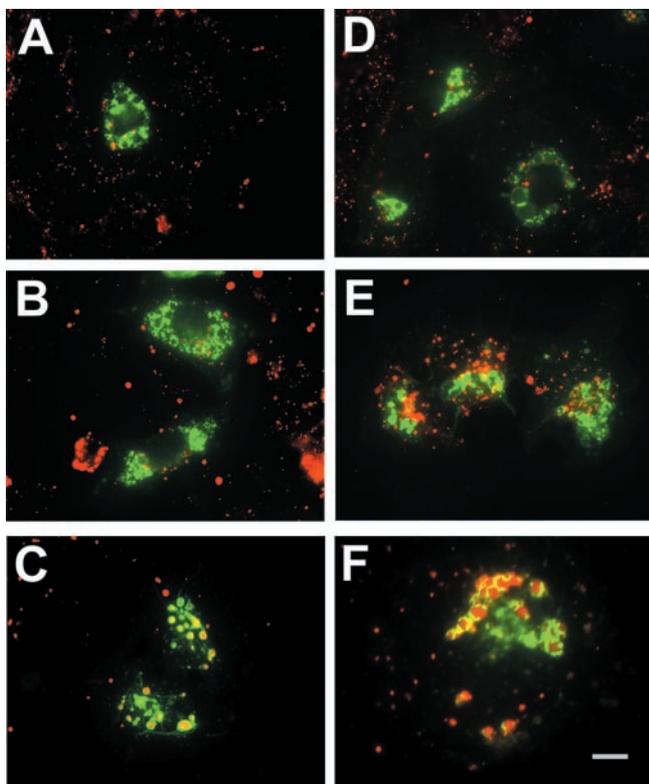
nylpropylamino)benzoic acid] and DIDS, and is never seen in untransfected cells (20). Each of these characteristics is identical to what has been reported for the highly homologous ClC-5 and ClC-4 (8).

In contrast, the currents that we reported to be associated with expression of the long form of ClC-3 (32), as well as the properties of ClC-3 that have been observed by Duan et al. (3), are quite different from those of ClC-4 and ClC-5. They have only weak outward rectification, are sensitive to both NPPB and DIDS, and are identical to endogenous currents that are present in untransfected cells. We thus believe that the currents that we previously observed associated with the long form of ClC-3 (32) were endogenous to the cells and were not mediated by ClC-3 itself. In subsequent experiments in which greater care has been taken to prevent cell swelling, we no longer see plasma membrane currents associated with expression of ClC-3 long form.

It is important to note that we have only been able to observe wild-type ClC-3 currents in transiently transfected cells that possess large intracellular vesicles. We have not been able to observe ClC-3 currents in transfected cells without intracellular vesicles. We suggest that the presence of vesicles indicates an extreme degree of ClC-3 overexpression. Only in this case does enough of the channel appear on the plasma membrane to produce measurable whole cell currents. The long form of ClC-3 is also expressed well in our transient transfection assays, but it does not form vesicles. Our inability to see currents with this molecule may reflect more efficient intracellular retention.

These findings need to be understood in the context of other recent studies of ClC-3. As discussed in detail previously (20), our results differ markedly from those of Duan et al. (3) and Kawasaki et al. (16). We find that ClC-3 appears to be an intracellular channel that contributes to acidification of intracellular vesicles and is not activated by cell swelling. However, our results are entirely compatible with the recent studies of Stobrawa et al. (35), who used knockout mice and confirmed that ClC-3 is not associated with swelling-activated currents. These authors also observed abnormalities of acidification in synaptic vesicles of hippocampal neurons. Synaptic vesicles share some membrane protein components with lysosome-related organelles such as melanosomes and platelet-dense granules (2, 26). Thus the observations of Stobrawa et al. are compatible with a role of ClC-3 in promoting acidification of lysosomes in other cell types. Our results are also partially consistent with the recent paper by Weylandt et al. (39), who confirmed that ClC-3 is primarily intracellular and is not a swelling-activated channel. However, Weylandt et al. obtained a different voltage dependence than we did, with much more conduction at negative voltages. The explanation for this difference is not clear. It could reflect a difference in cell systems with specific regulatory proteins present only in some cell types. Huang et al. (13) also studied ClC-3 in stably transfected cells. They observed a Ca^{2+}-dependent Cl^- current that was weakly outward

rectifying and sensitive to DIDS. The rectification and inhibitor sensitivity of these currents are different from what we see for ClC-3, but we have not examined Ca^{2+} dependence in our system. Another difference between our work and that of Huang et al. is that ClC-3 channels were open constitutively in our experiments but required elevated Ca^{2+} to become open in the studies of Huang et al.

Several alternative explanations for our results also need to be considered. The possibility exists that the vesicles result from some effect of overexpressed ClC-3 that is not related to its channel function. For example, this could be a nonspecific effect of membrane protein overexpression, or the introduction of ClC-3 into these cells could alter vacuolar H^+-ATPase expression levels. Several facts can be used to argue against these possibilities. First, the E224A mutant is structurally identical to ClC-3 wild type except for the loss of a single-charged residue in the channel pore. It was abundantly expressed in CHO-K1 cells and appeared to have similar intracellular localization, but it did not produce vesicle enlargement. In addition, overexpression of other similar molecules such as ClC-3 long form does not produce these vesicles (Fig. 1). Second, vacuolar H^+-ATPase is expressed in multiple intracellular compartments (11). If the primary effect of ClC-3 were to increase its expression, the observed effects would not be selective for lysosomes.

An important issue concerning ClC-3, ClC-4, and ClC-5 is how the extreme outward rectification (8, 20) is compatible with channel function in any real cellular compartment, where the cytosolic potential is always negative. In most cells, cytosol positive potentials, which would allow ion conduction, never occur in either the plasma membrane or in any conceivable intracellular organelle. This problem is so significant as to suggest that the main function of ClC-3 might not involve its ion channel activity. However, our study demonstrated intracellular Cl^- fluxes into ClC-3-containing vesicles (Fig. 6). ClC-3, therefore, does function as an intracellular channel. One possible explanation is suggested by the recent determination of the crystal structure of the bacterial ClC channel by Dutzler et al. (4). This structure reveals that a COOH-terminal α-helix (the R helix) is oriented with its NH_2 terminus in the pore selectivity filter and its COOH terminus in the cytosol. As suggested by Dutzler et al., binding of an accessory protein to the cytoplasmic COOH-terminal domain of the protein could alter the confirmation of the selectivity filter and modify the voltage dependence of ClC-3. In this scenario, failure to conduct Cl^- at negative voltages at the plasma membrane could keep the channel closed in the plasma membrane. Because the vesicles of the secretory and endocytic pathways do indeed fuse with the plasma membrane, it is inevitable that some ClC-3 will appear on the plasma membrane. However, the absence of the appropriate accessory proteins in plasma membrane would effectively close any ClC-3 channel molecules that appear there, helping to ensure that ClC-3 functions exclusively as an intracellular channel. This explanation is, of course,

speculative, and the exact purpose of the extreme outward rectification has yet to be determined. Further experiments are required to clarify this point.

We therefore conclude that ClC-3 functions as a Cl$^-$ channel in lysosome membranes and contributes to vesicular acidification. This finding is consistent with the demonstrated function of other members of the ClC family, particularly ClC-5 (12, 29). Mutations in ClC-7 also result in a defect in acidification by osteoclasts that leads to abnormal bone resorption (17). We may thus cautiously generalize that this class of intracellular Cl$^-$ channels is involved in a diverse array of intracellular acidification processes. It cooperates with vacuolar H$^+$-ATPase to allow acidification and vacuolation to occur. We believe this is the first demonstration of functional activity of ClC-3 in non-neuronal cells. Additional expression in other cell lines or observations in native cells is needed to understand further details of ClC-3 function.

REFERENCES

1. **Bodily K, Wang Y, Roman R, Sostman A, and Fitz JG.** Characterization of a swelling-activated anion conductance in homozygous typing cell hepatoma cells. *Hepatology* 25: 403–410, 1997.
2. **Dell'Angelica EC, Mullins C, Caplan S, and Bonifacino JS.** Lysosome-related organelles. *FASEB J* 14: 1265–1278, 2000.
3. **Duan D, Winter C, Cowley S, Hume JR, and Horowitz B.** Molecular identification of a volume-regulated chloride channel. *Nature* 390: 417–421, 1997.
4. **Dutzler R, Campbell EB, Cadene M, Chait BT, and MacKinnon R.** X-ray structure of a ClC chloride channel at 3.0 A reveals the molecular basis of anion selectivity. *Nature* 415: 287–294, 2002.
5. **Eliassi A, Garneau L, Roy G, and Sauvé R.** Characterization of a chloride-selective channel from rough endoplasmic reticulum membranes of rat hepatocytes: evidence for a block by phosphate. *J Membr Biol* 159: 219–229, 1997.
6. **Fahlke C, Yu HT, Beck CL, Rhodes TH, and George AL Jr.** Pore-forming segments in voltage-gated chloride channels. *Nature* 390: 529–532, 1997.
7. **Feranchak AP, Fitz JG, and Roman RM.** Volume-sensitive purinergic signaling in human hepatocytes. *J Hepatol* 33: 174–182, 2000.
8. **Friedrich T, Breiderhoff T, and Jentsch TJ.** Mutational analysis demonstrates that ClC-4 and ClC-5 directly mediate plasma membrane currents. *J Biol Chem* 274: 896–902, 1999.
9. **Fukuda M.** Lysosomal membrane glycoproteins. Structure, biosynthesis, and intracellular trafficking. *J Biol Chem* 266: 21327–21330, 1991.
10. **George AL Jr, Bianchi L, Link EM, and Vanoye CG.** From stones to bones: the biology of ClC chloride channels. *Curr Biol* 11: R620–R628, 2001.
11. **Grabe M and Oster G.** Regulation of organelle acidity. *J Gen Physiol* 117: 329–344, 2001.
12. **Gunther W, Luchow A, Cluzeaud F, Vandewalle A, and Jentsch TJ.** ClC-5, the chloride channel mutated in Dent's disease, colocalizes with the proton pump in endocytotically active kidney cells. *Proc Natl Acad Sci USA* 95: 8075–8080, 1998.
13. **Huang P, Liu J, Di A, Robinson NC, Musch MW, Kaetzel MA, and Nelson DJ.** Regulation of human CLC-3 channels by multifunctional Ca^{2+}/calmodulin-dependent protein kinase. *J Biol Chem* 276: 20093–20100, 2001.
14. **Jentsch TJ, Friedrich T, Schriever A, and Yamada H.** The CLC chloride channel family. *Pflügers Arch* 437: 783–795, 1999.
15. **Jentsch TJ and Gunther W.** Chloride channels: an emerging molecular picture. *Bioessays* 19: 117–126, 1997.
16. **Kawasaki M, Suzuki M, Uchida S, Sasaki S, and Marumo F.** Stable and functional expression of the ClC-3 chloride channel in somatic cell lines. *Neuron* 14: 1285–1291, 1995.
17. **Kornak U, Kasper D, Bosl MR, Kaiser E, Schweizer M, Schulz A, Friedrich W, Delling G, and Jentsch TJ.** Loss of the ClC-7 chloride channel leads to osteopetrosis in mice and man. *Cell* 104: 205–215, 2001.
18. **Lerat H, Honda M, Beard MR, Loesch K, Sun J, Yang Y, Okuda M, Gosert R, Xiao SY, Weinman SA, and Lemon SM.** Steatosis and liver cancer in transgenic mice expressing the structural and nonstructural proteins of hepatitis C virus. *Gastroenterology* 122: 366–375, 2002.
19. **Li XH and Weinman SA.** Chloride channels and hepatocellular function. Prospects for molecular identification. *Annu Rev Physiol* 64: 13.1–13.25, 2002.
20. **Li X, Shimada K, Showalter LA, and Weinman SA.** Biophysical properties of ClC-3 differentiate it from swelling-activated chloride channels in CHO-K1 cells. *J Biol Chem* 275: 35994–35998, 2000.
21. **Lin HJ, Herman P, Kang JS, and Lakowicz JR.** Fluorescence lifetime characterization of novel low-pH probes. *Anal Biochem* 294: 118–125, 2001.
22. **Maglova LM, Jackson AM, Meng XJ, Carruth MW, Schteingart CD, Ton-Nu HT, Hofmann AF, and Weinman SA.** Transport characteristics of three fluorescent conjugated bile acid analogs in isolated rat hepatocytes and couplets. *Hepatology* 22: 637–647, 1995.
23. **Meng XJ and Weinman SA.** Cyclic AMP and swelling activated chloride conductance in rat hepatocytes. *Am J Physiol Cell Physiol* 271: C112–C120, 1996.
24. **Morier N and Sauvé R.** Analysis of a novel double-barreled anion channel from rat liver rough endoplasmic reticulum. *Biophys J* 67: 590–602, 1994.
25. **Mullins C and Bonifacino JS.** The molecular machinery for lysosome biogenesis. *Bioessays* 23: 333–343, 2001.
26. **Mullins C, Hartnell LM, and Bonifacino JS.** Distinct requirements for the AP-3 adaptor complex in pigment granule and synaptic vesicle biogenesis in Drosophila melanogaster. *Mol Gen Genet* 263: 1003–1014, 2000.
27. **Nelson N and Harvey WR.** Vacuolar and plasma membrane proton-adenosinetriphosphatases. *Physiol Rev* 79: 361–385, 1999.
28. **Nordeen MH, Jones SM, Howell KE, and Caldwell JH.** GOLAC: an endogenous anion channel of the Golgi complex. *Biophys J* 78: 2918–2928, 2000.
29. **Piwon N, Gunther W, Schwake M, Bosl MR, and Jentsch TJ.** ClC-5 Cl$^-$-channel disruption impairs endocytosis in a mouse model for Dent's disease. *Nature* 408: 369–373, 2000.
30. **Sanchez-Olea R, Fuller C, Benos D, and Pasantes-Morales H.** Volume-associated osmolyte fluxes in cell lines with or without the anion exchanger. *Am J Physiol Cell Physiol* 269: C1280–C1286, 1995.
31. **Schmid SL.** Toward a biochemical definition of the endosomal compartment. Studies using free flow electrophoresis. *Subcell Biochem* 19: 1–28, 1993.
32. **Shimada K, Li XH, Xu GY, Nowak DE, Showalter LA, and Weinman SA.** Expression and canalicular localization of two isoforms of the ClC-3 chloride channel from rat hepatocytes. *Am J Physiol Gastrointest Liver Physiol* 279: G268–G276, 2000.
33. **Steinmeyer K, Klocke R, Ortland C, Gronemeier M, Jockusch H, Grunder S, and Jentsch TJ.** Inactivation of muscle chloride channel by transposon insertion in myotonic mice. *Nature* 354: 304–308, 1991.
34. **Steinmeyer K, Schwappach B, Bens M, Vandewalle A, and Jentsch TJ.** Cloning and functional expression of rat CLC-5, a chloride channel related to kidney disease. *J Biol Chem* 270: 31172–31177, 1995.
35. **Stobrawa SM, Breiderhoff T, Takamori S, Engel D, Schweizer M, Zdebik AA, Bosl MR, Ruether K, Jahn H, Draguhn A, Jahn R, and Jentsch TJ.** Disruption of ClC-3, a

chloride channel expressed on synaptic vesicles, leads to a loss of the hippocampus. *Neuron* 29: 185–196, 2001.

36. **Tilly BC, Mancini GM, Bijman J, van Gageldonk PG, Beerens CE, Bridges RJ, De Jonge HR, and Verheijen FW.** Nucleotide-activated chloride channels in lysosomal membranes. *Biochem Biophys Res Commun* 187: 254–260, 1992.

37. **Van Dyke RW.** Acidification of lysosomes and endosomes. *Subcell Biochem* 27: 331–360, 1996.

38. **Wagner S, Deymeer F, Kurz LL, Benz S, Schleithoff L, Lehmann-Horn F, Serdaroglu P, Ozdemir C, and Rudel R.** The dominant chloride channel mutant G200R causing fluctuating myotonia: clinical findings, electrophysiology, and channel pathology. *Muscle Nerve* 21: 1122–1128, 1998.

39. **Weylandt KH, Valverde MA, Nobles M, Raguz S, Amey JS, Diaz M, Nastrucci C, Higgins CF, and Sardini A.** Human ClC-3 is not the swelling-activated chloride channel involved in cell volume regulation. *J Biol Chem* 276: 17461–17467, 2001.

40. **Wills NK and Fong P.** ClC chloride channels in epithelia: recent progress and remaining puzzles. *News Physiol Sci* 16: 161–166, 2001.